JOURNAL OF MATERIALS SCIENCE 29 (1994) 5383–5389

Liquid-phase sintering of chemically unstable silicon carbide–lithium/magnesium aluminosilicate–titania composites

Z. PÁNEK
Institute of Inorganic Chemistry, Slovak Academy of Sciences, Dúbravská cesta 9, 842 36 Bratislava, Slovakia

The fully dense 55 wt % SiC–45 wt % (LAS/MAS/TiO_2) composite consisting of SiC filler particles and glassy matrix has been prepared by liquid-phase sintering in the presence of carbon, using the heating rate of 800 °C min^{-1}, the maximum sintering temperature 1600 °C and the nitrogen overpressure of 8×10^{-5} Pa applied at a maximum particle mobility stage. The total liquid-phase sintering time did not exceed 4 min. The bloating effect was always observed in the carbon-free atmosphere during liquid-phase sintering.

1. Introduction

Ceramic materials can be fabricated using a substantially higher amount of liquid during sintering if final properties fulfil the conditions of technical applications. The theoretical background for such a method of powder consolidation is described elsewhere [1–7]. Nearly poreless ceramics can be prepared at approximately 30–40 vol % liquid by particle rearrangement (PR) alone [1, 2]. A post-sintering crystallization treatment is usually performed to improve the mechanical properties of a sintered body by the transformation of glass into crystalline phases [8–10].

General advantages of this consolidation method are the low temperature and short sintering time as well as a possible tailoring of microstresses in the material. However, problems during sintering and crystallization can be expected if some chemical reactions, particularly gas-forming reactions or evaporation, change the chemical and phase composition of the sintered body.

Cordierite, $2MgO{\cdot}2Al_2O_3{\cdot}5SiO_2$ (MAS) and spodumene, $Li_2O{\cdot}Al_2O_3{\cdot}4SiO_2$ (LAS) as glass matrix-forming compounds, titania as the nucleation aid and silicon carbide as the particle filler, have been selected as a system in which the above-mentioned problems exist. In this system, the oxidation of SiC [11, 12] at high temperatures and oxygen pressures is expected, as shown by Reaction 1

$$SiC(s) + CO_2(g) + O_2(g) \rightleftharpoons SiO_2(s, l) + 2CO(g) \quad (1)$$

$$K_1(1600\ K) = 1.1 \times 10^{22}$$

where K_1 is the calculated equilibrium constant of Reaction 1 using data from Barin and Knacke [13]. At low oxygen pressure, particularly in the presence of carbon, the reduction of SiO_2 to gaseous SiO is possible by the reaction

$$SiO_2(s) + C(s) \rightleftharpoons SiO(g) + CO(g) \quad (2)$$

$$K_2 = 3.1 \times 10^{-5}(1600\ K) - 7.7 \times 10^{-2}(1900\ K)$$

The strong exchange reaction between TiO_2 and SiC in the presence of MAS has been reported elsewhere [14].

The aim of present work was to show that nearly poreless composite structures can be prepared from the powder of a chemically unstable non-oxide–oxide system by liquid-phase sintering during rapid heating in an appropriate atmosphere.

2. Experimental procedure

Analytical grade oxides, except for lithium (Li_2CO_3) were used for the synthesis of the powder matrix. Two α-SiC powders with different median particle size $d_{50} = 0.7$ μm (HCST A 20, Germany and $d_{50} = 4.6$ μm (Ventron − 325 mesh, Germany, milled in-house) were used as the particle filler. The glass matrix powder containing MAS and LAS in the weight ratio 1:1 and 4.5 wt % TiO_2 was prepared by melting in a platinum crucible at 1400 °C for 2 h in air and subsequent quenching in water and attrition milling (SiC milling media). The $d_{50} = 2.2$ μm was determined for the matrix powder by the sedimentation method. No crystalline phases were detected in the matrix powder by the XRD method. The density of glass ($\rho = 2.56$ g cm^{-3}, $\sigma = 0.015$) as well as the density of samples after densification, was measured by Archimedes' method.

The composite powder mixtures were prepared by dispersing required amounts of SiC and glass powder in acetone and mixing in a polyethylene bottle with agate balls for 48 h. The dried, homogeneous powder mixture was pressed in a steel die into pellets of 6 mm diameter and approximately 5 mm high at a pressure of 100 MPa. Two sets of composite mixtures, labelled S and V, were prepared from the powdered SiC HCST A 20 and SiC Ventron, respectively. The SiC filler content was either 55, 57 or 60 wt % (corresponding to the 50.6, 48.6 and 45.5 vol % glass, respectively) for both sets. The porosities of the green pellets were

0022–2461

42% ± 0.6% and 45% ± 0.7% for mixtures S and V, respectively.

The heating microscope (Leitz, Germany) was used for direct observation of sintering, as well as for measurement of the wetting angle between the liquid matrix and SiC by the sessile drop method. Pellets of the composite mixture or pure matrix, placed on a SiC monocrystal platelet, were heated in an alumina vacuum-tight tube without carbon contamination at a heating rate of 40–1000 °C min^{-1} in static air (10^5 Pa) and at 40 °C min^{-1} in static nitrogen or argon (both 10^5 Pa) or in vacuum (10^2 Pa) up to 1600 °C.

The technical-grade nitrogen and argon gases containing approximately 0.01 vol % impurities (mainly O, H_2O) were used for all experiments.

In order to monitor the linear dimensional change of pellets as a function of temperature, heating rate, time and gas pressure up to 2×10^5 Pa under a uniaxially applied pressure of about 7×10^2 Pa, a vertical dilatometer with a graphite sample holder and heating element was used. For dilatometry, the sample was placed between boron nitride discs to avoid direct contact with the graphite.

The majority of the sintering experiments was performed in vacuum, nitrogen or argon within the pressure range 10^2–8×10^5 Pa at a heating rate of 25–800 °C min^{-1} up to 1600 °C in a graphite resistance vacuum-overpressure furnace using a graphite crucible as a sample holder. The samples placed on the boron nitride platelet were quenched after different stages of sintering, and subsequently analysed.

The weight difference, density, phases present (XRD) and microstructure (optical microscopy, SEM) were determined for each sample. Some samples were analysed by electron probe microanalysis (EPMA) JXA850-KEVEX. The nitrogen content of some sintered samples was determined by the modified Kjeldahl method as described elsewhere [15].

3. Results and discussion

3.1. Chemical aspect of sample bloating and yielding

The results of wetting angle and sintering measurements which were performed in the heating microscope in the absence of carbon at a pressure of 10^5 Pa, confirm the existence of bloating (see Fig. 1) in the SiC–LAS/MAS–TiO_2 system above the solidus temperature (~ 1330 °C) regardless of the atmosphere and heating rate. The bloating intensity increases with increasing temperature and decreases depending on the atmosphere in the following sequence: air, argon, nitrogen, vacuum. Such behaviour seems surprisingly prominent in air, for which the following short explanation may be given. From the observed bloating of a liquid-matrix drop on an SiC monocrystal platelet in air, it was deduced that in addition to Reaction 1, which prevails on the free SiC surface, the following gas-forming reactions [11]

$$SiC(s) + 2SiO_2(l) \rightleftharpoons 3SiO(g) + CO(g) \quad (3)$$

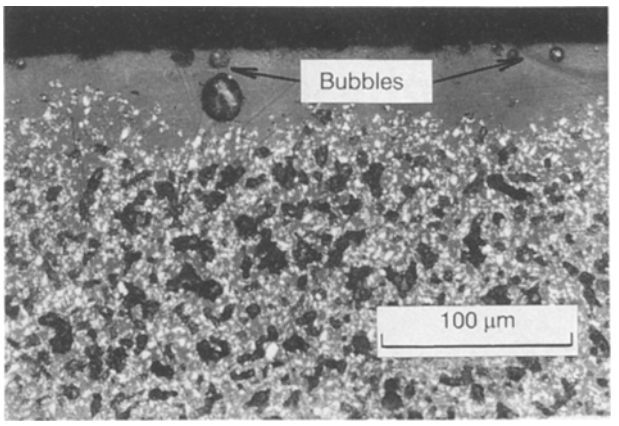

Figure 1 Optical micrograph of a polished section of sample V containing 55 wt % SiC after heating at 1500 °C for 1 min in air and subsequent quenching.

$$K_3(1900\,K) = 4.2 \times 10^{-5}$$
$$SiC(s) + \text{“}SiO_2\text{”}\ (melt) + H_2O(g) \rightleftharpoons$$
$$2SiO(g) + CO(g) + H_2(g) \quad (4)$$
$$K_4(1900\,K)\ F = 2.9$$

must be taken into account at the interface between SiC and the liquid matrix. Hence, in addition to the thermal expansion of entrapped gas, a new gas may originate in the solid–liquid interface. This gas is responsible for bloating and makes measurements of wetting angle impossible.

The same chemical reactions as in Reactions 1, 3 and 4 take place during the sintering in air, due to the high reaction surface of green pellets; Reaction 1 overlaps Reactions 3 and 4. Therefore, a weight gain 3%–6%, depending on the experimental conditions, was determined after densification in air. Supposing that only oxidation of SiC (Reaction 1) is responsible for the weight gain, then the calculated conversion of SiC to SiO_2 is 11%–22%, indicating that the amount of liquid as well as the SiO_2 content in the liquid, increase considerably so that yielding of the sample was observed during sintering.

Regarding the main impurities in nitrogen or argon (O, H_2O) and a possible contamination of the sample by carbon, Reactions 1–4 also describe the chemical behaviour during densification in argon or nitrogen. However, contrary to the situation in air, Reactions 2–4 are dominant here. This is confirmed by the weight loss of all samples sintered in nitrogen or argon. The weight loss is accompanied by a lowering of the liquid content. The maximum lowering of the liquid content may be expected if Reaction 2 prevails in addition to Reactions 7, 8, 11–13 (see later).

3.2. Effect of filler loading and heating rate on LPS

The effect of filler loading on the densification of S and V samples in argon and nitrogen is shown in Fig. 2a. The sintering was performed in the vacuum-overpressure furnace. The samples sintered in air were not evaluated because the strong bloating and liquid-content increase made the measurement of shrinkage

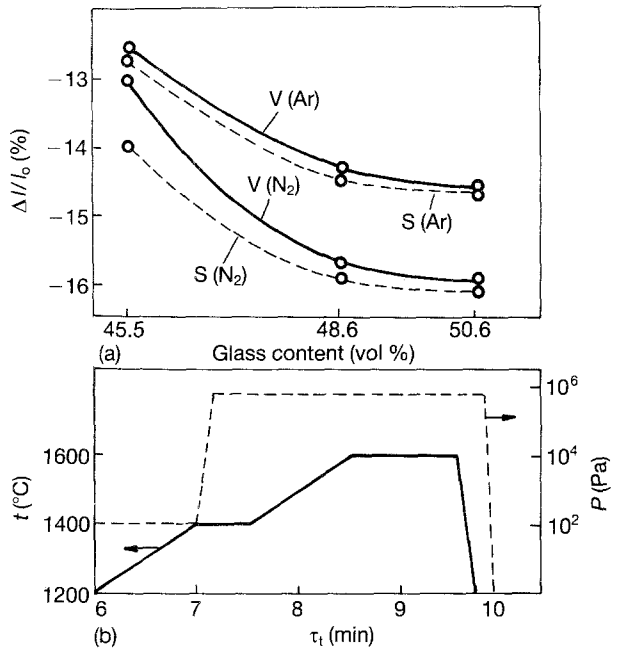

Figure 2 Dependence of shrinkage on filler loading and atmosphere for samples S and V (a) after the temperature–pressure treatment according to the schedule shown in (b).

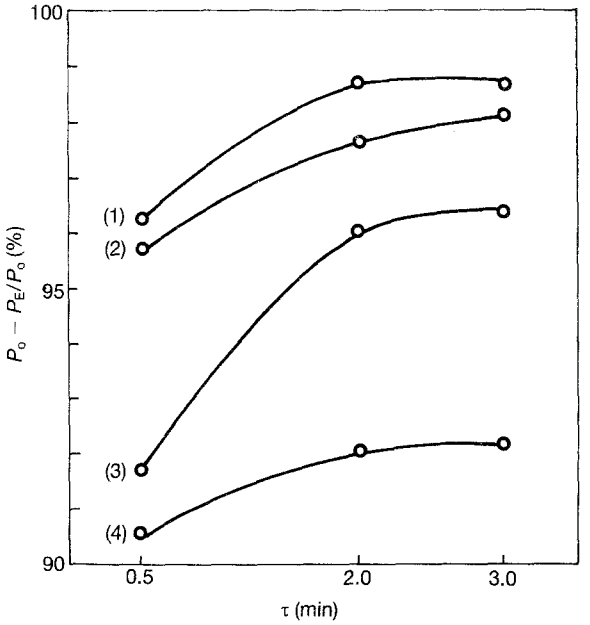

Figure 3 Dependence of final densification $(P_0 - P_f)/P_0$ of samples V on dwell time at 1600 °C under 8×10^5 Pa nitrogen after different heating rates 1–4 between 1300 and 1600 °C under 10^5 Pa nitrogen heating rate in vacuum up to 1300 °C was 400 °C min^{-1}, for all samples. (1) 400 °C min^{-1}, (2) 200 °C min^{-1}, (3) 50 °C min^{-1}, (4) 25 °C min^{-1}. P_0, P_f, green body and final porosity, respectively.

impossible. The considerably higher shrinkage in nitrogen and significantly higher shrinkage for finer filler particle were determined after a temperature–pressure treatment as shown in Fig. 2b. The highest shrinkage densities without shape deformation were achieved for 55 wt % SiC (50.6 vol % glass), therefore this composition was chosen for further investigation.

The dependences of densification of 55 SiC/45 glass pellets (calculated density $\rho = 2.892$ g cm^{-3}) on the time dwell at maximum sintering temperature for different heating rates are shown in Fig. 3. The weight loss after 3 min dwell ranges from 1.5–3 wt % for the highest and lowest heating rate, respectively. It is difficult to explain the lowest densification in Fig. 3 by only the liquid-content lowering of about 1.5 %. Moreover, it must be taken into account, that the longest PR period exists at the lowest heating rate between 1300 and 1600 °C; therefore, a higher degree of PR could be expected after this period (see also densification step I in Fig. 7). However, an opposite final effect has been observed as shown in Fig. 3. These results support the suggestion, that densification at a high liquid content is influenced more by the heating rate than by a small lowering of liquid content.

During the sintering at a very low heating rate, a low temperature gradient also exists, and vice versa for an indirect heating method. It may be assumed, that depending on the actual thermal conductivity and heating rate, the time which is necessary to achieve the solidus temperature in the core of a body, considering zero time at the moment of solidus temperature on the surface, may be longer in the case of very low heating rate. If this assumption is correct, a high degree of liquid redistribution [6, 16] and PR in the outer part is achieved before the liquid is formed in the core of a sintered body at a very low heating rate. Then it may be difficult to rearrange the already arranged, more densely packed "skin" particles with regard to the "core" particles, because a liquid redistribution and disruption of some liquid bridges in the skin area are necessary. This can lead to increased final porosity if insufficient external force is applied. The above mentioned consideration may also be expressed as follows: for a better densification during the LPS, it is advantageous for the rate of liquid formation from the surface to the core of a body to be faster than the rate of PR in the same direction. In particular, at higher liquid content during sintering (high PR rate), the heating rate is a very important parameter as is seen in Figs 3–6.

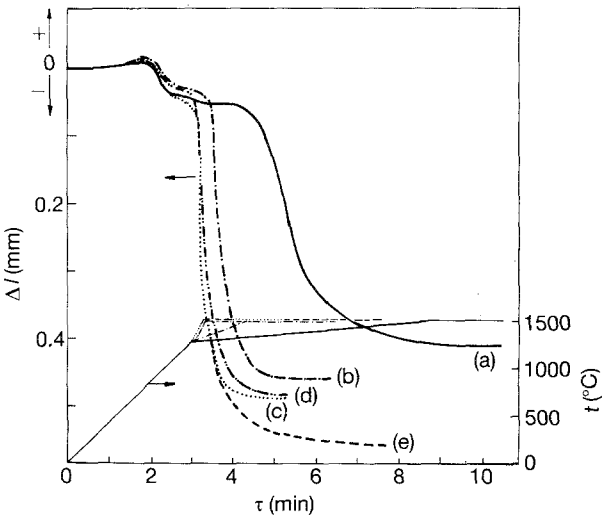

Figure 4 Dependence of dilatometric curves of samples V on different heating rates in the temperature range 1200–1500 °C in (—, — · —, · · ·) vacuum (10^5 Pa), (— · · —) argon (10^5 Pa), and (– – –) nitrogen (10^5 Pa). (a) 50 °C min^{-1}, (b) 200 °C min^{-1}, (c) 800 °C min^{-1}, (d) 800 °C min^{-1}, (e) 800 °C min^{-1}.

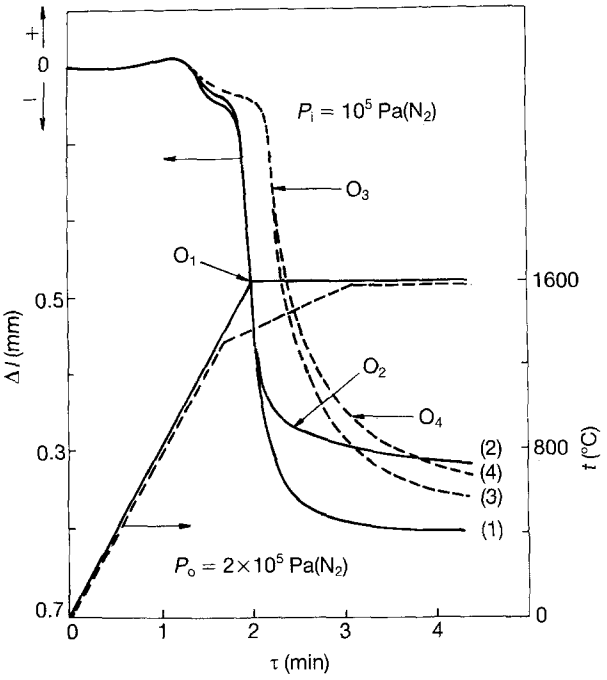

Figure 5 Dependence of dilatometric curves of samples V on different nitrogen overpressures set up at points O_1–O_4 at two heating rates: (——) 800 °C min^{-1}, (— — —) 200 °C min^{-1}. p_i initial pressure; p_0 final pressure.

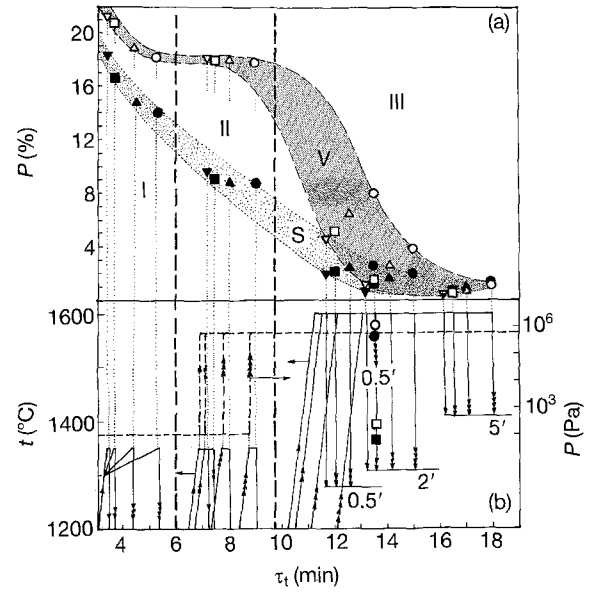

Figure 6 Dependence of porosity of samples (▽, □, △, ○) V and (▼, ■, ▲, ●) S on temperature–pressure treatment (a) which was divided into three steps according to the schedule shown in (b); (▽ ▼) 400 °C min^{-1}, (□, ■) 200 °C min^{-1}, (△, ▲) 50 °C min^{-1}, (○ ●) 25 °C min^{-1}; overpressure gas, nitrogen.

The dilatometer and overpressure furnace were used to evaluate the influence of heating rate, overpressure and atmosphere on sintering. The results of dilatometric measurements are shown in Figs 4 and 5. It was determined that under the same experimental conditions, except heating rate, the highest shrinkage or density always corresponded to the highest heating rate, regardless of the atmosphere used (see also Fig. 6). The weight losses of samples for which results are shown in Figs 4–6 did not exceed 2 wt %. For the sake of clarity, only dilatometric curves belonging to the measurements in vacuum at the different heating rates are depicted in Fig. 4. All these results indicate, that at a very high heating rate, in addition to the better conditions for liquid redistribution and PR, the deleterious influence of gas-forming reactions and evaporation is suppressed as a consequence of different reaction and densification kinetics.

3.3. Effect of atmosphere on LPS

A significant difference exists between the shrinkage which was achieved in argon or in nitrogen (Figs 2 and 4). All other experimental parameters were kept constant. Such behaviour can be explained as follows: the oxygen and water vapour impurities in both gases are relatively high and similar, so that in the presence of carbon (heating element, crucible, etc.) its transport from hot to colder parts is expected, e.g. due to the carbon monoxide disproportionation according to the reaction

$$2CO(g) \rightleftharpoons C(s) + CO_2(g) \quad (5)$$

$$K_5 = 2.9\times10^{-4}(1600\text{ K}) - 4.2\times10^{-5}(1900\text{ K})$$

Hence, a carbon contamination of the sample must be taken into account. Under such rather strong reduction conditions, particular reactions expressed by

$$SiO(g) + C(s) \rightleftharpoons Si(s, l) + CO(g) \quad (6)$$

$$K_6 = 4.8\ (1600 - 1900\text{ K})$$

$$SiO_2(s, l) + 3C(s) \rightleftharpoons SiC(s) + 2CO(g) \quad (7)$$

$$K_7 = 9.2\times10^{-2}(1600\text{ K}) - 10.7(1900\text{ K})$$

$$TiO_2(s) + 3C(s) \rightleftharpoons TiC(s) + 2CO(g) \quad (8)$$

$$K_8 = 3.2(1600\text{ K}) - 1.5\times10^3(1900\text{ K})$$

can take place in the sintered body. Moreover, in the presence of carbon, the equilibrium oxygen pressure (p_0^{eq}) of the system metal (Ti, Si) –C–O determined by the reaction

$$2CO(g) \rightleftharpoons 2C(s) + O_2(g) \quad (9)$$

$$p_0^{eq}(9) = 2\times10^{-16}(1550\text{ °C}) - 5\times10^{-16}(1600\text{ °C})$$

is lower than (p_0^{eq} of SiO_2 at a temperature above 1550 °C (see values of p_0^{eq} in Reaction 10). Therefore, the direct reduction of SiO_2 according to

$$SiO_2(s) \rightleftharpoons Si(l) + O_2(g) \quad (10)$$

$$p_0^{eq}(10) = 2\times10^{-16}(1550\text{ °C}) - 10^{-15}(1600\text{ °C})$$

is possible at a temperature above 1550 °C. Similarly, the direct reduction of TiO_2 is thermodynamically possible above 1620 °C. A small number of fine (about 1μm), rounded, very reflective grains was observed by optical microscopy (see Fig. 9). These grains were determined to be titanium by electron probe microanalysis (EPMA). No pure silicon grains were detected by the same method. Thus, either silicon is not formed or reacts with carbon and/or nitrogen. However, the nitrogen-containing compounds were not determined by the XRD method in the sintered samples.

During the period of open porosity, gas exchange between the pores and the ambient atmosphere is

possible; therefore, Reactions 2–10 run towards the right-hand side. This is accompanied by a lowering of the total liquid content and a change in chemical composition of the liquid. However, the main contribution to the total weight loss, which ranges from 0.8–5 wt % depending on the atmospheric pressure, heating rate and time dwell at maximum temperature, seems to be caused by evaporation of SiO. This is supported by the decrease in the silicon content, determined in the sintered samples by EPMA, which is in a good accordance with the total weight loss.

In the nitrogen atmosphere, the reactions

$$3SiO(g) + 2N_2(g) + C(s) \rightleftharpoons Si_3N_4(s) + 3CO(g) \quad (11)$$

$$K_{11}(1900\ K) = 1.6 \times 10^7$$

$$3Si(l) + 2N_2(g) \rightleftharpoons Si_3N_4(s) \quad (12)$$

$$K_{12}(1900\ K) = 6.3 \times 10^2$$

$$Si(l) + SiO(g) + N_2(g) \rightleftharpoons Si_2N_2O(s)[17] \quad (13)$$

$$K_{13}(1900\ K) = 1.7 \times 10^4$$

are possible. By analogy, Reactions 11 and 12 may be written for titanium. These reactions could play an important role, particularly after the pores are closed. They are accompanied by a lowering of the nitrogen pressure as well as the total gas pressure in the pores and by the conversion of gas and liquid to solid. The pore-pressure lowering effect, as well as the corresponding gas/liquid to solid conversion, positively influenced the densification. It follows from Reactions 11–13 that this effect increases as the overpressure increases. Such an effect does not exist in argon. Owing to the absence of gas-consuming reactions the lower final shrinkage (density) was always determined after densification in argon. Hence, the influence of nitrogen overpressure on the sintered body has two (physical and chemical) aspects.

Some dissolution of nitrogen [18] in the lithium/magnesium aluminosilicate melt may be expected, but neither this nor the solubility of argon was investigated in the present work. After densification, 0.5–4 wt % nitrogen were determined in the quenched samples, but no distinction was made between the nitrogen chemically bonded in solid phases or dissolved in the melt. The positive influence of nitrogen, compared to argon, on the sintering of the SiC–LAS/MAS–TiO_2 system above the solidus temperature was confirmed unambiguously.

3.4. Effect of gas overpressure on LPS

The dependence of shrinkage on the overpressure effect applied at the early or later stage of particle rearrangement is shown in Fig. 5. A higher shrinkage was always observed after the overpressure which was applied during the early stage of rearrangement (corresponding approximately to a maximum shrinkage rate) i.e. at the stage of relatively high porosity. Such behaviour indicates that, after liquid redistribution or in the early stage of particle rearrangement, the pore closure in the outer layer, and probably also in the core of a body, is finished or is in a mature stage

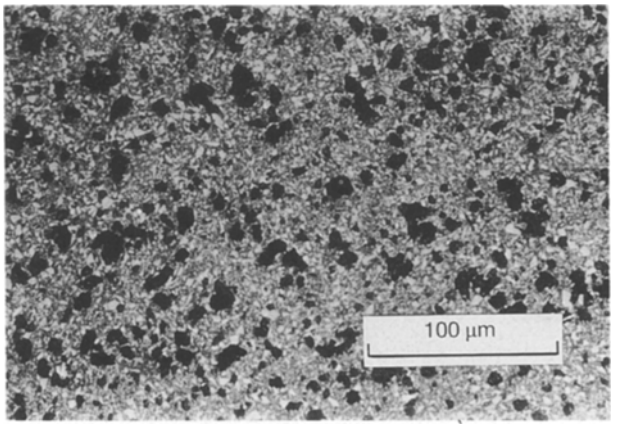

Figure 7 Optical micrograph of a polished section of sample V quenched from 1600 °C, immediately before overpressure was set up (corresponding to point O_1 in Fig. 5).

despite the high porosity, provided that a sufficiently high liquid content is present in a sintered body. The microstructure shown in Fig. 7 represents the state immediately before the overpressure application. Under increasing pressure the pores become smaller, which can lead to the disruption of some liquid bridges which allows a further particle rearrangement [16]. This overpressure effect has a lower efficiency if the pressure increase begins at a later stage of particle rearrangement, because the system is more rigid.

3.5. Effect of filler and matrix particle size on LPS at different heating rates

Fig. 6 shows the porosities of samples S and V as a function of the temperature–pressure treatment for three steps of densification. For each mixture, S and V, and each heating rate, the three samples were prepared by the same procedure using densification steps I and II. A different heating rate, ranging from 25–400 °C min^{-1}, was used in densification step I. Densification step II (overpressure introduced) was identical for all samples so that the heating rate in step I was the only variable before step III. Hence, step III in Fig. 6 expresses the porosity as a function of heating rate in step I and dwell time at the maximum sintering temperature 1600 °C under a pressure of 8×10^5 Pa of nitrogen. In the step III, the first sample was sintered for 0.5 min at maximum sintering temperature, the second one for 2 min and the third one for 5 min. Each sample was quenched after each densification step and the density of the samples was determined. The values of final porosity were comparable and low, but the densification paths for the mixtures labelled S and V differed considerably.

After the first densification step, the lowest porosities were determined at the lowest heating rate (and vice versa) as a consequence of the longer heating time above the solidus temperature, indicating that a higher degree of particle rearrangement was achieved. At a high liquid content the attractive forces which act among the particles are similar for different interparticle distance, and increase as the particle size increases [19]. Therefore, it is impossible to explain the

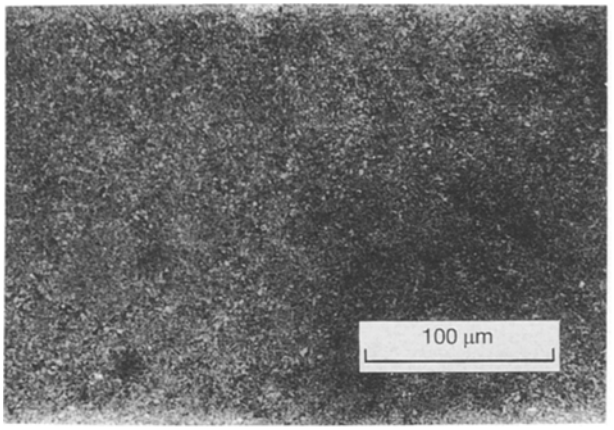

Figure 8 Optical micrograph of a polished section of sample S after LPS (heating rate 800 °C min^{-1}, $p_i = 10^5$ Pa, $p_f = 8 \times 10^5$ Pa, overpressure set up at 1570 °C, dwell time at 1600 °C, 2 min).

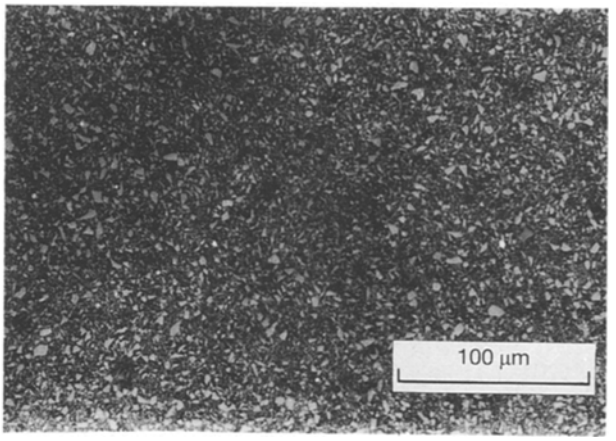

Figure 9 Optical micrograph of a polished section of sample V after LPS; LPS parameters as in Fig. 8.

porosity difference after step I by the interparticle forces. The porosity difference between mixtures S and V may be explained by the different SiC and matrix particle size. The different particle arrangement of a green body concerning the liquid-forming particles and filler particles, seems to be responsible for the porosity difference (after step I) provided that the filler/matrix volume ratio is approximately 1. The coarser glass particles (compared to the SiC) form a major part of the skeleton in mixture S, whereas SiC particles prevail in the skeleton of mixture V. A higher mobility of the particle system above the solidus temperature is thus expected in mixture S, because the solid skeleton is transformed to liquid.

The increased porosity difference between S and V samples after step II (Fig. 6) is probably related to the different degree of closed porosity before a gas overpressure was set up, and a more difficult rearrangement of coarser particles at a relatively high viscosity. The lower overpressure effects for samples V support this explanation.

As the sintering temperature increases (stage III), the physico-chemical properties of the melt and interfaces change, and particularly the viscosity decrease contributes to the intensive final particle rearrangement (Fig. 6). Expect for the highest heating rate, the porosities are even lower in the case of sample V. This repeatedly confirms the advantage of the presence of an overpressure at a more "rearrangeable state", provided that a closed porosity exists in the sintered body at the moment the overpressure is set up. From the facts that more gas is entrapped in samples labelled V (higher porosity) before step III of the densification and that the final porosities of samples V are the same or slightly higher than the porosities of samples S, the positive effect of gas-consuming reactions seems evident.

The microstructures of samples S and V are shown in Figs 8–10 and demonstrate a very low final porosity.

Further research will be directed to the crystallization of glassy matrix and evaluation of microstresses in crystallized material.

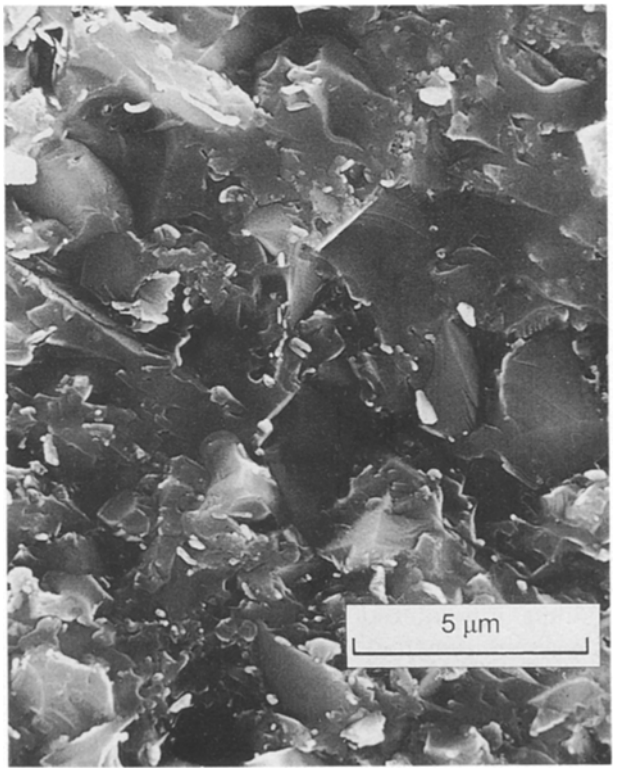

Figure 10 Scanning electron micrograph of a fracture surface of sample V (same sample as in Fig. 9).

4. Conclusions

1. It has been impossible to achieve a high density material from a powder SiC–LAS/MAS–TiO_2 system by particle rearrangement during a pressureless LPS in an oxidizing or neutral atmosphere.

2. A considerable increase of liquid content during sintering in air and the opposite effect in a reducing, carbon-containing atmosphere, was observed.

3. It was confirmed that the following conditions positively influence the particle rearrangement during LPS: (a) the highest possible heating rate, (b) the presence of carbon which provides a reduction atmosphere, (c) a reactive gas atmosphere (nitrogen), and (d) the presence of *in situ* formed substances (SiO, Ti, Si) which react with the gas.

4. Under the sintering conditions mentioned above a fully dense composite material based on the SiC–LAS/MAS–TiO_2 system has been prepared.

5. Based on the results achieved, it can be deduced that a direct "temperature gradient-less" heating method will be advantageous for LPS compared with an indirect heating method.

Acknowledgement

This work was supported in part by the Slovak Grant Agency for Science (grant 2/999435/93).

References

1. W. D. KINGERY, *J. Appl. Phys.* **30** (1950) 301.
2. *Idem, ibid.* **30** (1950) 307.
3. R. M. GERMAN, "Liquid Phase Sintering" (Plenum Press, New York, 1985).
4. T. M. SHAW, *J. Am. Ceram. Soc.* **69** (1986) 27.
5. R. B. HEADY and J. W. CAHN, *Metall. Trans.* **1** (1970) 185.
6. K. G. EWSUK and L. W. HARRISON, in "Sintering of Advanced Ceramics", edited by C. A. Handwerker, J. E. Blendell and W. A. Kaysser (American Ceramic Society, Columbus, OH, 1990) p. 436.
7. O.-H. KWON, PhD thesis, Pennsylvania State University (1986).
8. K. M. PREWO, J. J. BRENNAN and G. K. LAYDEN, *Am. Ceram. Soc. Bull.* **65** (1986) 305.
9. H. SCHEIDLER and E. RODEK, *ibid.* **68** (1989) 1926.
10. L. R. PINCKNEY, in "Engineered Materials Handbook", Vol. 4 "Ceramics and Glasses" Volume Chairman, S.J. Schneider Jr. (ASM International, 1991) p. 433.
11. R. R. SICKAFOOSE Jr and D. W. REAEY, *J. Am. Ceram. Soc.* **76** (1993) 316.
12. S. C. FRAMER, C. DELLACORTE and P. O. BOOK, *J. Mater. Sci.* **28** (1993) 1147.
13. I. BARIN and O. KNACKE, "Thermochemical properties of inorganic substances" (Springer-Verlag, Berlin, Heidelberg, New York, 1973).
14. W. PANNHORST, M. SPALLEK, R. BRÜCKNER, H. HEGELER, C. REICH, G. GRATHWOHL, B. MEIER and D. SPELMANN, *Ceram. Eng. Sci. Proc.* **11** (1990) 947.
15. T. LIČKO and P. ŠAJGALÍK, *Ceramics-Silikáty* **35** (1991) 127.
16. V. SMOLEJ, S. PEJOVNIK and W. A. KAYSSER, *Powder Metal. Int.* **14** (1982) 34.
17. M. BRUCE FEGLEY Jr, *J. Am. Ceram. Soc.* **64** (1981) C 124.
18. E. A. DANCY and D. JANSSEN, *Can. Metall. Q.* **15** (1976) 103.
19. Z. PÁNEK, *Sci. Sintering* **16** (1984) 13.

Received 11 August 1993
and accepted 22 April 1994